Letter

Singlet, triplet, and mixed all-to-all pairing states emerging from incoherent fermions

Jagannath Sutradhar [1,2,*] Jonathan Ruhman [2] and Avraham Klein [1]
[1]*Physics Department, Ariel University, Ariel 40700*
[2]*Department of Physics, Bar-Ilan University, Ramat Gan 5290002, Israel*

(Received 15 April 2024; accepted 23 September 2024; published 4 November 2024)

The electron-electron and electron-phonon coupling in complex materials can be more complicated than simple density-density interactions, involving intertwined dynamics of spin, charge, and spatial symmetries. This motivates studying universal models with complex interactions and whether BCS-type singlet pairing is still the "natural" fate of the system. To this end, we construct a Yukawa-SYK model with nonlocal couplings in both spin and charge channels. Furthermore, we provide for time-reversal-symmetry breaking dynamics by averaging over the Gaussian unitary ensemble rather than the orthogonal ensemble. We find that the ground state of the system can be an orbitally nonlocal superconducting state arising from incoherent fermions with no BCS-like analog. The superconductivity has an equal tendency to triplet and singlet pairing states separated by a non-Fermi liquid phase. We further study the fate of the system within the superconducting phase and find that the expected ground state, away from the critical point, is a mixed singlet/triplet state. Finally, we find that, while at T_c the triplet and singlet transitions are dual to one another, below T_c the duality is broken, with the triplet state more susceptible to orbital fluctuations just by its symmetry. Our results indicate that such fluctuation-induced mixed states may be an inherent feature of strongly correlated materials.

DOI: 10.1103/PhysRevResearch.6.L042036

Introduction. One of the best-known avenues to analyze superconductivity beyond the classic Bardeen-Cooper-Schrieffer (BCS) paradigm of weakly coupled Fermi liquids is studying toy models of fermions coupled to a soft boson [1–15]. The boson encodes both the dynamics and the symmetry properties of the interaction. Of particular focus has been the fate of such models when approaching a quantum critical point (QCP), such that the diverging correlation length creates both long-ranged and strong pairing interactions and drives the fermions incoherent. An overwhelming majority of studies consider *spin-singlet* pairing [11–15]. This is probably because most known superconductors are singlets and the most common pairing mediators with the simplest symmetry properties (e.g., phonons) tend to prefer singlet pairing [16].

In truth, though, sufficiently complex materials should host interactions with intertwined attraction and repulsion [17–19], involving both charge and spin [20,21], as well as fluctuations that break lattice, time-reversal [22,23], and inversion symmetries [20,24–26]. Such interactions have been considered for a host of candidate materials [17–22,24–32]. For example, Fe-based superconductors near antiferromagnetic order [17,18,33] have been proposed to arise from spin fluctuations that locally break time-reversal symmetry. In addition, a variety of superconducting systems appear to evince phenomena that are neither clearly singletlike nor tripletlike, raising the question of how likely mixed singlet/triplet states are in these systems [25,34–38]. This motivates finding a universal model of strongly correlated pairing that is "agnostic" as regards spin singlet and triplet pairing, as well as various space-time and lattice symmetries. With such a model one can study the properties of strongly correlated superconductors, investigate whether spin singlet and triplet pairing have equal footing or not, and look for exotic pairing states that might be missing in "garden-variety" models.

In this Letter, we develop and study such a model. Our starting point is a Yukawa-Sachdev-Ye-Kitaev (Y-SYK) model [13,32,39], where N fermions are randomly coupled to M bosons in $0+1$D, as shown in Fig. 1(a). This model is analytically solvable in the large-N large-M limit and exhibits both non-Fermi liquid (NFL) behavior and high-temperature superconductivity. We consider both spin and charge coupling, with independent coupling constants, g_z and g_0, respectively. Moreover, we allow for time-reversal-symmetry (TRS) breaking fluctuations by drawing the coupling matrix from the Gaussian unitary ensemble (GUE), rather than the more usual orthogonal ensemble (GOE).

We find that upon lowering the temperature the bosons become critical and the NFL becomes unstable to an *interorbital* pairing state $\Phi \sim \langle c_i c_j \rangle$, $i \neq j$ [Fig. 1(c)], where i, j denote orbitals and we suppressed spin indices. Such pairing is qualitatively distinct from the "standard" BCS type $\Phi \sim \langle c_i c_i \rangle$ that arises in the GOE averaging [Fig. 1(b)]. Furthermore, this nonlocal state is tuned between triplet and singlet pairing depending on the relative coupling strengths as shown in the phase diagram Fig. 1(d). An NFL phase separates the two

*Contact author: sutradj@biu.ac.il

Published by the American Physical Society under the terms of the Creative Commons Attribution 4.0 International license. Further distribution of this work must maintain attribution to the author(s) and the published article's title, journal citation, and DOI.

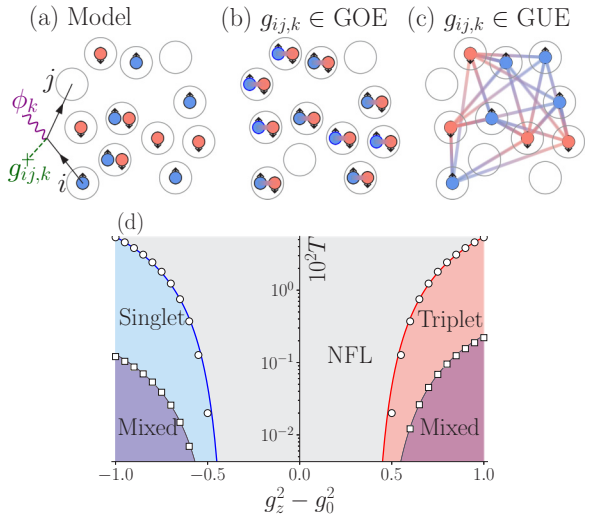


FIG. 1. (a) Schematic of the model Hamiltonian [Eq. (1)]: N spinful fermionic orbitals (circles) coupled to M bosons (wiggly line) via random coupling $g_{ij,k}$, scattering electrons between orbitals i and j. The scattering occurs in both density (σ^0) and spin (σ^z) channels with variances g_0^2 and g_z^2. (b) Earlier studies averaged $g_{ij,k}$ over the GOE, leading to intraorbital singlet pairing. (c) In our study, $g_{ij,k}$ is drawn from the GUE, resulting in an "all-to-all" interorbital pairing between all possible up-down spin pairs. (d) The phase diagram showing dual triplet and singlet SC phases, terminating at QCPs and separated by an NFL phase. At $T < T_c$, both singlet and triplet phases can induce a coexisting singlet/triplet state, with the SC ground state transiting to a mixed pairing state. The dots represent a numerical solution of the gap equation and the lines depict a fit to our analytical results; see the text for further details.

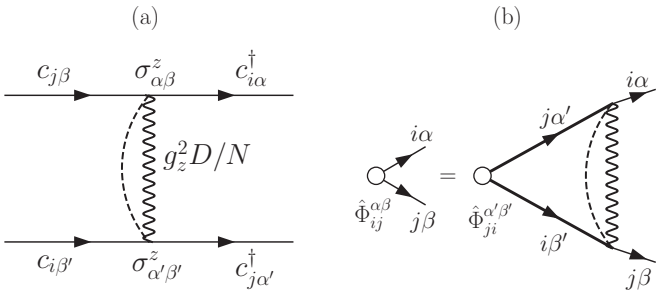


FIG. 2. Feynman diagrams. (a) Schematic of the interacting four-fermionic term mediated by the bosonic propagator D (wavy line) after disorder average represented by the dashed line. (b) The linearized gap equation. Note that the exchange in ij indices in $\hat{\Phi}$ on the right side makes one of the triplet channels attractive.

phases. We also study the pairing state below T_c. We find that the low-T pairing state is generically a nonlocal triplet-singlet mixture. Our results show that the previously deemed NFL phase can become unstable to pairing once the nonlocal state is considered. This includes models where the random couplings are a sum of two random numbers drawn from the GOE and GUE [13].

Thus systems with both charge and spin fluctuations have a rich landscape of superconducting phases that go beyond the usual paradigms of unconventional superconductivity and can involve not just broken symmetries such as time reversal, but also spatially nonlocal correlations even at the mean-field level. In these systems, an introduction of nonlinear contributions plays a crucial role in shaping the phase diagram, even in the absence of static symmetry breaking. We describe our model and results in detail below.

Model. We consider M bosonic fields, ϕ_k, randomly coupled to N fermions $c_{i\alpha}$ as schematically depicted in Fig. 1(a) and expressed as

$$H = H_z + H_0 + \sum_k \left(\pi_k^2 + m_0^2 \phi_k^2\right),$$

$$H_a = 1/\sqrt{MN} \sum_{ijk\alpha\beta} g^a_{ij,k} \phi_k c^\dagger_{i\alpha} \sigma^a_{\alpha\beta} c_{j\beta} \quad (a = z, 0), \qquad (1)$$

where π_k are the momenta fields conjugate to ϕ_k and α, β are spin indices. The random couplings $g^a_{ij,k}$ are completely uncorrelated between the spin and charge components, denoted by $a = z, 0$, respectively. The interaction form is chosen to allow for universal spin and charge fluctuations, while avoiding stability issues that arise from SU(2) spin fluctuations [21,40]. The couplings are drawn from the GUE, such that the average of the real and imaginary parts $\overline{\mathrm{Re}(g^a_{ij,k})\mathrm{Re}(g^a_{i'j',k'})} = g_a^2 \delta_{kk'}(\delta_{ii'}\delta_{jj'} + \delta_{ij'}\delta_{ji'})$ and $\overline{\mathrm{Im}(g^a_{ijk})\mathrm{Im}(g^a_{i'j'k'})} = g_a^2 \delta_{kk'}(\delta_{ii'}\delta_{jj'} - \delta_{ij'}\delta_{ji'})$, respectively, and g_a is the coupling strength. Note that the complex $g^a_{ij,k}$ manifestly breaks TRS, which is restored upon disorder averaging. Previous studies considered a similar model with TRS by drawing the coupling from the GOE. In that case, there is a large-N instability towards an intraorbital singlet pairing phase characterized by the nonvanishing expectation value $\sum_i \langle c^\dagger_{i\uparrow} c^\dagger_{i\downarrow}\rangle \neq 0$. In contrast, the GUE-averaged action avoids the intraorbital pairing and opens a path to more exotic pairing states. The distinct pairing forms are illustrated in Figs. 1(b) and 1(c).

Triplet normal state and pairing instability. Before jumping into the full Hamiltonian in Eq. (1), we start by focusing on the spin fluctuation H_z, which governs the triplet pairing, and set $g_0 = 0$. We then show that the complimentary singlet pairing scenario where $g_z = 0$, $g_0 \neq 0$ can be obtained directly from the triplet case. Finally, we study the interplay between both spin and charge couplings.

As usual, we disorder average the partition function associated with the Hamiltonian in Eq. (1) with $H_0 = 0$ using the replica trick and consider only the replica-diagonal term in the action [32]. The form of the interacting part of the action is

$$\mathcal{S}_I \sim -g_z^2 \sum_{k,i,\ldots} \int d\tau\, \phi_k c^\dagger_{i\alpha} \sigma^z_{\alpha\beta} c_{j\beta} \int d\tau' \phi_k c^\dagger_{j\alpha'} \sigma^z_{\alpha'\beta'} c_{i\beta'} \qquad (2)$$

[see the Supplemental Material (SM) [41] for details] and the corresponding Feynman diagram is shown in Fig. 2(a). Superficially, Eq. (2) appears similar to "standard" spin-fermion interactions whose QC dynamics have been studied extensively [11–15,42,43]. However, the interaction in H_z of Eq. (1) involves both spin flips *and* nonlocality, very different from the usual on-site magnetic interactions, giving rise to some nontrivial physics. In what follows we study the fate of the fermions in the presence of this interaction.

Connecting different legs in Fig. 2(a) we obtain the self-energies in the large N, M limit. The Green's function is diagonal both in orbital and spin basis (SM [41]) and it is defined as $G(\omega_n) = 1/[\mathrm{i}\omega_n + \mathrm{i}\Sigma(\omega_n)]$. At finite T, the electronic self-energy is given by

$$\Sigma(\omega_n) = \mathrm{i}g_z^2 T \sum_m D(\omega_n - \omega_m)\frac{1}{2}\mathrm{Tr}[\sigma^z G(\omega_m)\sigma^z], \quad (3)$$

where $\omega_n = (2n+1)\pi T$, $n \in \mathbb{Z}$ are fermionic Matsubara frequencies, and Tr represents trace over the spin indices. $D(\Omega_n) = [\Omega_n^2 + m_0^2 + \Pi(\Omega_n)]^{-1}$ is the bosonic propagator. The bosonic self-energy is given by

$$\Pi(\Omega_n) = 2g_z^2 T \frac{N}{M} \sum_m \mathrm{Tr}[\sigma^z G(\omega_m + \Omega_n)\sigma^z G(\omega_m)], \quad (4)$$

where $\Omega_n = 2n\pi T$ are the bosonic Matsubara frequencies. Similar to what occurs in previously studied models (see, e.g., Refs. [5,7,9,13,39,44–47]), Eqs. (3) and (4) give rise to NFL behavior, with $\Sigma(\omega) \sim \mathrm{sgn}(\omega)|\omega|^{(1-\eta)/2}$ and $\Pi(\Omega) - \Pi(0) \sim g^2|\Omega|^\eta$ at low T, ω, and self-tuned criticality that renormalizes the boson mass to exactly zero. The exponent η varies from 0 to 1 as a function of N/M (SM [41]).

The form of the interaction naturally leads us to consider an interorbital pairing state $\Phi_{ij}^{\alpha\beta} = \langle c_{i\alpha}^\dagger c_{j\beta}^\dagger \rangle$, which includes all possible orbital pairs. A somewhat similar type of pairing was considered in Ref. [39]. The linearized equation for the interorbital order parameter, depicted in Fig. 2(b), is given by

$$\hat{\Phi}_{ij}^{\alpha\beta}(\omega_n) = \frac{g_z^2}{N} T \sum_{m,\alpha',\beta'} D(\omega_n - \omega_m)\sigma_{\alpha\alpha'}^z \times G(\omega_m)\hat{\Phi}_{ji}^{\alpha'\beta'}(\omega_m)G(-\omega_m)\sigma_{\beta\beta'}^z. \quad (5)$$

Note the orbital exchange $i \leftrightarrow j$ between the left- and right-hand side of the equation, which is a consequence of the discussed nonlocality. The antisymmetry of the pairing function is enforced by the orbital exchange, i.e., $\hat{\Phi}_{ij}^{\alpha\beta} = -\hat{\Phi}_{ji}^{\alpha\beta}$. Consequently, Eq. (5) indicates attraction only when $\hat{\Phi}_{ij}^{\alpha\beta} = \hat{\Phi}_{ij}\sigma_{\alpha\beta}^x$, which signifies a triplet pairing state. Note that this is the *only* attractive channel, with the other two spin channels, as well as the singlet channel, being repulsive. This contrasts starkly with quantum critical models with a local spin-fermion interaction, where each magnetic channel attracts two spin channels and repels the third [21]. To simplify Eq. (5), we neglect the orbital phase fluctuation and consider $\hat{\Phi}_{ij} = \Phi_t A_{ij}$, where Φ_t is the amplitude of the pairing function dependent only on frequency and A_{ij} is a skew-symmetric matrix, such that all elements $A_{i>j} = 1$, $A_{i<j} = -1$, and $A_{i=j} = 0$. Choosing a different antisymmetric matrix A_{ij} yields the same results (SM [41]). We will discuss the origin and consequence of this degeneracy later on.

At $T = 0$ Eq. (5) has a SC instability in the regime $\sqrt{2M} > N$ and in the large M and N limit [5,13,39]. In contrast to the BCS theory, for $\sqrt{2M} < N$ even strong attraction does not lead to SC. At finite T, the bosons develop a mass correction and the pairing equation resembles that in Ref. [13]. The critical temperature (T_c) for the phase transition from the NFL to SC follows $T_c \sim g_z^2$ (SM [41]).

Singlet channel and mixed case. We next consider the pure singlet case, $g_z = 0$, $g_0 \neq 0$; the gap equation exhibits attraction in the singlet channel, characterized by the pairing function $\hat{\Phi}_{ij}^{\alpha\beta} = \mathrm{i}\Phi_s S_{ij}\sigma_{\alpha\beta}^y$, where S is a symmetric traceless matrix. As before, we neglect the fluctuations and set all the off-diagonal elements of the matrix to be 1, $S_{ij} = 1 - \delta_{ij}$ (SM [41]). The normal state and SC gap equations remain the same as in the triplet case. Consequently, the phase diagram resembles the earlier case, replacing the triplet SC with a singlet SC. Thus, above the critical $\sqrt{M}/N$ ratio, the ground state for our model with either of the couplings is always SC arising from within the incoherent NFL state. This is again in contrast with the case of GOE averaging, where the BCS-type local pairing sets in at the same energy scale as NFL physics [13,32]. For the singlet case, a BCS-type local pairing $\hat{\Phi}_{ij}^{\alpha\beta} \propto \delta_{ij} i\sigma_{\alpha\beta}^y$ is degenerate with the nonlocal pairing. For simplicity, we consider henceforth only the nonlocal state, since it keeps the physics qualitatively the same (SM [41]).

We are now ready to consider the full Hamiltonian of Eq. (1). As $g_{ij,k}^0$ and $g_{ij,k}^z$ are uncorrelated, the interacting part of the disorder averaged action is a sum of two terms similar to Fig. 2(a): one for σ^z as earlier and another for σ^0, with their respective strengths g_z and g_0. The normal state solution remains NFL. Within the linearized gap equation, there is a critical strength λ_c of $\lambda = |g_z^2 - g_0^2|$ beyond which the SC phase emerges. The state is either singlet (for $g_0 > g_z$) or triplet (for $g_z > g_0$), with no mixing [see Fig. 1(d)]. The critical temperature follows $T_c \sim \exp(-\pi/\sqrt{\lambda - \lambda_c})$ [13] (SM [41]). Between the SC phases, the system remains an NFL down to $T = 0$.

Solution of the gap equation below T_c. To explore the phase diagram at $T < T_c$ we must turn to the nonlinear gap equation. First, let us consider the case with only one finite coupling, σ^z or σ^0. Obtaining an analytic solution to the full nonlinear equations is challenging due to the form of the matrices A and S, which couple all orbitals. However, near T_c, we can study the first nonlinear correction to the linearized gap equation by dressing one of the Green's functions in the diagram Fig. 2(b)

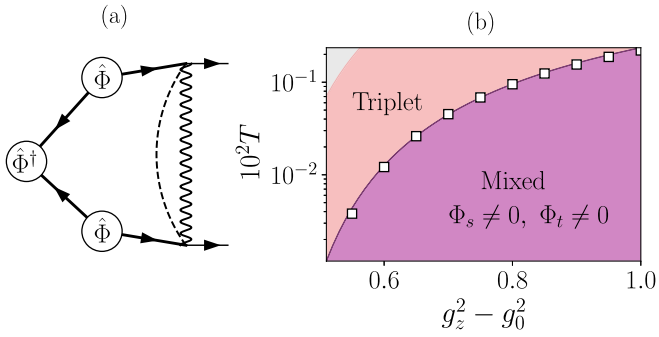


FIG. 3. Nonlinearity in the gap equation. (a) The Feynman diagram represents the first nonlinear term in the expansion of the gap equation. (b) Variation of the critical temperature $T_{t\to m}$ to the mixed state as a function of $g_z^2 - g_0^2$. This figure zooms at the segment of Fig. 1(d) depicting the transition from the triplet to the mixed state. The squares denote the numerical data points and the dashed line represents a fitting to the curve $T_{t\to m} \sim \exp[-\pi/(\sqrt{\lambda - \lambda_c})]$ (SM [41]) for $g_0^2 = 1$.

with a correction of order $\sim|\Phi_{t(s)}(\omega_m)|^2\Phi_{t(s)}(\omega_m)$, as depicted in Fig. 3(a) (SM [41]). The nonlinear term has an opposite sign compared to the linear term [Eq. (6)] and leads to the usual $\Phi_{t(s)} \sim \sqrt{T_c - T}$ behavior.

It is important to note that while orbital phase fluctuations is inconsequential at the linear level [Eq. (5)], it is expected to influence the nonlinear solution. However, given the complexity involved, we focus here on the homogeneous solution, which is a natural first step towards addressing the challenging problem.

We now turn to the case involving both σ^z and σ^0 couplings. We introduce a *mixed* pairing function $\hat{\Phi} = \Phi_t A\sigma^x + i\Phi_s S\sigma^y$. As mentioned earlier, at the linear approximation, Φ_t and Φ_s do not interact. However, higher-order terms introduce an interaction between Φ_t and Φ_s. The equation for $\Phi_{t(s)}$ can be written in simplified form as

$$\Phi_{t(s)}(\omega_n) \approx \left[g_{z(0)}^2 - g_{0(z)}^2\right]\frac{T}{N}\sum_m \frac{D(\omega_n-\omega_m)}{|\omega_m+\Sigma(\omega_m)|^2}\left[\Phi_{t(s)}(\omega_m) - \frac{\Phi_{t(s)}(\omega_m)}{|\omega_m+\Sigma(\omega_m)|^2}\left\{\zeta_{t(s)}\Phi_{t(s)}^2(\omega_m) + \frac{2}{3}\Phi_{s(t)}^2(\omega_m)\right\}\right], \tag{6}$$

where we rescaled $\Phi_{t(s)} \to \Phi_{t(s)}/N$ and neglected $1/N^2$ terms. The factor $\zeta_t = 1/3$ and $\zeta_s = 1$. We also took both fields to be real, since their phase turns out to be locked by the nonlinear terms (SM [41]).

The nonlinear term implies the emergence of a mixed pairing state at lower temperatures. For example, let us consider $g_z^2 > g_0^2$ and T just below T_c, which results in $\Phi_t \neq 0$ and $\Phi_s = 0$, i.e., the SC phase consists purely of triplet pairing. Now, in the equation for Φ_s the nonlinear contribution $\propto\Phi_t^2\Phi_s$ is attractive although the linear term is repulsive. Consequently, as we lower the temperature and $|\Phi_t|$ increases, the attraction at low frequencies dominates over the linear repulsive term, triggering a second instability below some critical T. Thus the SC phase becomes a superposition of singlet and triplet pairing. This mechanism is reminiscent of the competition between repulsive and attractive interactions in the Anderson-Morel model [48]. The arguments for $g_0^2 > g_z^2$ are exactly analogous and this gives rise to the phase diagram plotted in Fig. 1(d) for $\eta = 0.68$ and $N = 1$. We confirm our analysis by numerically determining the critical temperature $T_{t(s)\to m}$ (SM [41]). An analysis of the nonlinear gap equation within the SC phase reveals that the mixed state is stable all the way to the dominant order's critical point at $\lambda = \lambda_c$ and our numerics confirm this analysis. This contradicts the decoupling of the two states that occurs at the level of the linearized gap equation. Thus the QCP appears to be a singular point with different behavior depending on how it is approached in the phase diagram. This is probably because the Ginzburg-Landau expansion has coefficients that diverge at low temperatures. In the SM, we compute the next order terms in the Ginzburg-Landau expansion, showing that it has the form of an asymptotic series. To conclusively determine whether the QCPs to the single state and mixed state converge or not requires an analysis of the full gap equation, which is beyond the scope of this work. This is also true for any analysis of the mixed phase beyond the onset temperature.

The phase diagram Fig. 1(d) implies a duality between the singlet and triplet states. However, an interesting distinction exists between them. To understand it, we recall that the T_c obtained in the triplet state does not depend on the choice of the antisymmetric matrix A. The existence of a degeneracy is a manifestation of an S_N permutation symmetry of the disorder-averaged action Eq. (2). On the contrary, no such degeneracy exists in the singlet case, such that S is unique. Indeed, the matrix S forms a *one-dimensional* irreducible representation (irrep) of S_N, while A belongs to a multidimensional irrep, with $N(N-1)/2$ different elements. Nonetheless, it should be noted that the gap between the different irreps vanishes in the $N \to \infty$ limit.

Discussion. We have studied the Yukawa-SYK model for a random coupling between M bosons and N fermions drawn from the GUE, representing the absence of TRS. We couple the bosons to both spin and charge. The intraorbital pairing term vanishes upon averaging the random coupling (diagonal replica symmetry breaking). In the absence of this term, the leading pairing instability is a highly nonlocal interorbital pairing state with an equal superposition on all orbitals. By tuning the relative strength between the charge and spin couplings the ground state is tuned through a sequence of QCPs, separating between singlet, NFL, and triplet phases. Going deeper into each one of these phases, there is an additional transition to a singlet-triplet mixed state, as shown in the phase diagram Fig. 1(d).

It is interesting to compare the inter- and intraorbital pairing order parameters with the standard BCS pairing wave function in a finite-dimensional system with translational invariance (i.e., with a Fermi surface). In the BCS wave function, the pair correlations are between k and $-k$ and are therefore equivalent to intraorbital pairing. On the other hand, the interorbital order parameter we presented here would imply pairing correlations between all momentum states. Thus the wave function corresponding to the interorbital pairing state is inconsistent with the picture of momentum-space quasiparticles. In that sense, one may think of a GOE-averaged Y-SYK system as the quasiparticle weak coupling limit and the GUE averaged system as a strong coupling limit. Moreover, the existence of an instability in the entire phase diagram implies that the NFL phase driven by TRS breaking is generically unstable to pairing in the Y-SYK model.

It is also interesting that the triplet order parameter belongs to a *multidimensional* irreducible representation of the permutation group, while the singlet belongs to a one-dimensional irrep. Consequently, we expect the triplet state to be more susceptible to quantum fluctuations and thus the phase diagram in Fig. 1(d) will not retain the symmetry between the $g_z > g_0$ and $g_z < g_0$ limits where the transition into the triplet state will likely be suppressed. Furthermore, in the large-N limit, one may expect "pseudogap"-like physics, where phase coherence between the orders in the multidimensional subspace is destroyed.

Finally, the Y-SYK action has a $1+1$ AdS dual [49–52], where T_c is dual to an event horizon (indicating a black hole formation). Looking forward it is interesting to understand the gravity dual of the interorbital state found here. In particular, it may give access to black holes with finite angular momentum.

Acknowledgments. We thank J. Schmalian, A. V. Chubukov, S. K. Saha, and H. Yerzhakov for interesting discussions. A.K. and J.R. acknowledge support by the Israel Science Foundation (ISF) and the Israeli Directorate for Defense Research and Development (DDR&D) under Grant No. 3467/21.

[1] A. J. Millis, Effect of a nonzero temperature on quantum critical points in itinerant fermion systems, Phys. Rev. B **48**, 7183 (1993).

[2] A. Abanov and A. V. Chubukov, Spin-fermion model near the quantum critical point: One-loop renormalization group results, Phys. Rev. Lett. **84**, 5608 (2000).

[3] Z. Wang, W. Mao, and K. Bedell, Superconductivity near itinerant ferromagnetic quantum criticality, Phys. Rev. Lett. **87**, 257001 (2001).

[4] A. Abanov, A. V. Chubukov, and J. Schmalian, Quantum-critical superconductivity in underdoped cuprates, Europhys. Lett. **55**, 369 (2001).

[5] A. Abanov, A. V. Chubukov, and J. Schmalian, Quantum-critical theory of the spin-fermion model and its application to cuprates: Normal state analysis, Adv. Phys. **52**, 119 (2003).

[6] A. V. Chubukov and J. Schmalian, Superconductivity due to massless boson exchange in the strong-coupling limit, Phys. Rev. B **72**, 174520 (2005).

[7] Y. Wang, A. Abanov, B. L. Altshuler, E. A. Yuzbashyan, and A. V. Chubukov, Superconductivity near a quantum-critical point: The special role of the first Matsubara frequency, Phys. Rev. Lett. **117**, 157001 (2016).

[8] M. A. Metlitski, D. F. Mross, S. Sachdev, and T. Senthil, Cooper pairing in non-fermi liquids, Phys. Rev. B **91**, 115111 (2015).

[9] S. Raghu, G. Torroba, and H. Wang, Metallic quantum critical points with finite BCS couplings, Phys. Rev. B **92**, 205104 (2015).

[10] S. Lederer, Y. Schattner, E. Berg, and S. A. Kivelson, Superconductivity and non-Fermi liquid behavior near a nematic quantum critical point, Proc. Natl. Acad. Sci. USA **114**, 4905 (2017).

[11] G. Pan, W. Wang, A. Davis, Y. Wang, and Z. Y. Meng, Yukawa-SYK model and self-tuned quantum criticality, Phys. Rev. Res. **3**, 013250 (2021).

[12] W. Choi, O. Tavakol, and Y. B. Kim, Pairing instabilities of the Yukawa-SYK models with controlled fermion incoherence, SciPost Phys. **12**, 151 (2022).

[13] L. Classen and A. Chubukov, Superconductivity of incoherent electrons in the Yukawa Sachdev-Ye-Kitaev model, Phys. Rev. B **104**, 125120 (2021).

[14] W. Wang, A. Davis, G. Pan, Y. Wang, and Z. Y. Meng, Phase diagram of the spin-$\frac{1}{2}$ Yukawa–Sachdev-Ye-Kitaev model: Non-Fermi liquid, insulator, and superconductor, Phys. Rev. B **103**, 195108 (2021).

[15] D. Valentinis, G. A. Inkof, and J. Schmalian, BCS to incoherent superconductivity crossover in the Yukawa-Sachdev-Ye-Kitaev model on a lattice, Phys. Rev. B **108**, L140501 (2023).

[16] P. M. R. Brydon, S. Das Sarma, H.-Y. Hui, and J. D. Sau, Odd-parity superconductivity from phonon-mediated pairing: Application to $Cu_xBi_2Se_3$, Phys. Rev. B **90**, 184512 (2014).

[17] A. Chubukov, Pairing mechanism in Fe-based superconductors, Annu. Rev. Condens. Matter Phys. **3**, 57 (2012).

[18] D. J. Scalapino, A common thread: The pairing interaction for unconventional superconductors, Rev. Mod. Phys. **84**, 1383 (2012).

[19] D. Pimenov and A. Chubukov, Quantum phase transition in a clean superconductor with repulsive dynamical interaction, npj Quantum Mater. **7**, 45 (2022).

[20] L. P. Gor'kov and E. I. Rashba, Superconducting 2D system with lifted spin degeneracy: Mixed singlet-triplet state, Phys. Rev. Lett. **87**, 037004 (2001).

[21] A. V. Chubukov, A. M. Finkel'stein, R. Haslinger, and D. K. Morr, First-order superconducting transition near a ferromagnetic quantum critical point, Phys. Rev. Lett. **90**, 077002 (2003).

[22] A. Hinojosa, R. M. Fernandes, and A. V. Chubukov, Time-reversal symmetry breaking superconductivity in the coexistence phase with magnetism in Fe Pnictides, Phys. Rev. Lett. **113**, 167001 (2014).

[23] M. Khodas and A. V. Chubukov, Interpocket pairing and Gap symmetry in Fe-based superconductors with only electron pockets, Phys. Rev. Lett. **108**, 247003 (2012).

[24] E. Bauer, G. Hilscher, H. Michor, C. Paul, E. W. Scheidt, A. Gribanov, Y. Seropegin, H. Noël, M. Sigrist, and P. Rogl, Heavy fermion superconductivity and magnetic order in non-centrosymmetric $CePt_3Si$, Phys. Rev. Lett. **92**, 027003 (2004).

[25] P. A. Frigeri, D. F. Agterberg, A. Koga, and M. Sigrist, Superconductivity without inversion symmetry: MnsI versus $CePt_3Si$, Phys. Rev. Lett. **92**, 097001 (2004).

[26] J. A. Bert, B. Kalisky, C. Bell, M. Kim, Y. Hikita, H. Y. Hwang, and K. A. Moler, Direct imaging of the coexistence of ferromagnetism and superconductivity at the $LaAlO_3/SrTiO_3$ interface, Nat. Phys. **7**, 767 (2011).

[27] A. B. Vorontsov, M. G. Vavilov, and A. V. Chubukov, Interplay between magnetism and superconductivity in the iron pnictides, Phys. Rev. B **79**, 060508(R) (2009).

[28] J. Rech, C. Pépin, and A. V. Chubukov, Quantum critical behavior in itinerant electron systems: Eliashberg theory and instability of a ferromagnetic quantum critical point, Phys. Rev. B **74**, 195126 (2006).

[29] A. Klein and A. Chubukov, Superconductivity near a nematic quantum critical point: Interplay between hot and lukewarm regions, Phys. Rev. B **98**, 220501(R) (2018).

[30] W. Akbar, A. Biborski, L. Rademaker, and M. Zegrodnik, Topological superconductivity with mixed singlet-triplet pairing in moiré transition metal dichalcogenide bilayers, Phys. Rev. B **110**, 064516 (2024).

[31] H. Zhou, L. Holleis, Y. Saito, L. Cohen, W. Huynh, C. L. Patterson, F. Yang, T. Taniguchi, K. Watanabe, and A. F. Young, Isospin magnetism and spin-polarized superconductivity in Bernal bilayer graphene, Science **375**, 774 (2022).

[32] I. Esterlis and J. Schmalian, Cooper pairing of incoherent electrons: An electron-phonon version of the Sachdev-Ye-Kitaev model, Phys. Rev. B **100**, 115132 (2019).

[33] W.-C. Lee, S.-C. Zhang, and C. Wu, Pairing state with a time-reversal symmetry breaking in FeAs-based superconductors, Phys. Rev. Lett. **102**, 217002 (2009).

[34] A. Pustogow, Y. Luo, A. Chronister, Y.-S. Su, D. Sokolov, F. Jerzembeck, A. P. Mackenzie, C. W. Hicks, N. Kikugawa, S. Raghu *et al.*, Constraints on the superconducting order parameter in Sr_2RuO_4 from oxygen-17 nuclear magnetic resonance, Nature (London) **574**, 72 (2019).

[35] A. Ribak, R. M. Skiff, M. Mograbi, P. Rout, M. Fischer, J. Ruhman, K. Chashka, Y. Dagan, and A. Kanigel, Chiral superconductivity in the alternate stacking compound 4Hb-TaS_2, Sci. Adv. **6**, eaax9480 (2020).

[36] S. Salmani-Rezaie, K. Ahadi, and S. Stemmer, Polar nanodomains in a ferroelectric superconductor, Nano Lett. **20**, 6542 (2020).

[37] I. Hayes, T. Metz, S. Saha, J. Collini, N. Butch, D. Agterberg, A. Kapitulnik, and J. Paglione, Multicomponent superconducting order parameter in UTe_2, Science **373**, 797 (2021).

[38] M. Zegrodnik and A. Biborski, Mixed singlet-triplet superconducting state within the moiré $t-J-U$ model applied to twisted bilayer WSe_2, Phys. Rev. B **108**, 064506 (2023).

[39] Y. Wang, Solvable strong-coupling quantum-dot model with a non-fermi-liquid pairing transition, Phys. Rev. Lett. **124**, 017002 (2020).

[40] A. V. Chubukov and D. L. Maslov, Spin conservation and fermi liquid near a ferromagnetic quantum critical point, Phys. Rev. Lett. **103**, 216401 (2009).

[41] See Supplemental Material at http://link.aps.org/supplemental/10.1103/PhysRevResearch.6.L042036 for detailed calculations on both the normal state and the nonlinear pairing equations.

[42] Y.-M. Wu, A. Abanov, Y. Wang, and A. V. Chubukov, Interplay between superconductivity and non-Fermi liquid at a quantum critical point in a metal. II. the γ model at a finite t for $0 < \gamma < 1$, Phys. Rev. B **102**, 024525 (2020).

[43] Y.-M. Wu, S.-S. Zhang, A. Abanov, and A. V. Chubukov, Interplay between superconductivity and non-Fermi liquid behavior at a quantum-critical point in a metal. V. The γ model and its phase diagram: The case $\gamma = 2$, Phys. Rev. B **103**, 184508 (2021).

[44] B. L. Altshuler, L. B. Ioffe, and A. J. Millis, Low-energy properties of fermions with singular interactions, Phys. Rev. B **50**, 14048 (1994).

[45] V. Oganesyan, S. A. Kivelson, and E. Fradkin, Quantum theory of a nematic Fermi fluid, Phys. Rev. B **64**, 195109 (2001).

[46] W. Metzner, D. Rohe, and S. Andergassen, Soft Fermi surfaces and breakdown of Fermi-liquid behavior, Phys. Rev. Lett. **91**, 066402 (2003).

[47] L. Dell'Anna and W. Metzner, Fermi surface fluctuations and single electron excitations near Pomeranchuk instability in two dimensions, Phys. Rev. B **73**, 045127 (2006).

[48] P. Morel and P. W. Anderson, Calculation of the superconducting state parameters with retarded electron-phonon interaction, Phys. Rev. **125**, 1263 (1962).

[49] S. A. Hartnoll, C. P. Herzog, and G. T. Horowitz, Building a holographic superconductor, Phys. Rev. Lett. **101**, 031601 (2008).

[50] S. Sachdev, Bekenstein-Hawking entropy and strange metals, Phys. Rev. X **5**, 041025 (2015).

[51] J. Schmalian, Holographic superconductivity of a critical Fermi surface, arXiv:2209.00474.

[52] G.-A. Inkof, K. Schalm, and J. Schmalian, Quantum critical Eliashberg theory, the Sachdev-Ye-Kitaev superconductor and their holographic duals, npj Quantum Mater. **7**, 56 (2022).